



Obtention and characterization a vacuum-dried starch aerogel-type biomaterial from A98 rice (*Oryza sativa*)

E. Lozano-Pineda^a • R. Salgado-Delgado^{a*} • A. M. Salgado-Delgado^a • A. Olarte-Paredes^a • J. P. Hernández-Uribe^b • A. Vargas-Torres^b • E. García-Hernández^a • J. C. Gonzalez-Juarez^c

^aTecnológico Nacional de México, Instituto Tecnológico de Zacatepec. Zacatepec Morelos, México

^bUAEH, Instituto de Ciencias Agropecuarias, Tulancingo, Hidalgo. México

^cTecnológico Nacional de México, Instituto Tecnológico de Toluca. Metepec, Edo de México. México

Received 10 11 2022; accepted 01 16 2023

Available 12 31 2023

Abstract: In this work, aerogels were obtained by vacuum drying, an uncommon method that requires lower energy costs and creates materials with high porosity and small pore size. Starch from A98 rice was used, evaluating different concentrations (8, 10, and 12%) and retrogradation times (2, 4, and 6 days). The aerogels were characterized by analysis in a scanning electron microscope, in a Fourier transform infrared spectrophotometer and differential scanning calorimetry. Importantly, the retrogradation time showed no apparent significant changes in the formulation of the materials, and those created at a concentration of 10% presented a crystalline and amorphous reorganization. They were more homogeneous than the rest of the formulations while their pores measured 41 nm. Aerogels formulated with 8% presented higher swelling and water absorption but reduced solubility. The aerogels reported in this work show promising characteristics and the drying technique opens the doors to a more practical method that deserves further research.

Keywords: aerogel, starch, air drying, rice starch

*Corresponding author.

E-mail address: rene.sd@zacatepec.tecnm.mx (R. Salgado-Delgado).

Peer Review under the responsibility of Universidad Nacional Autónoma de México.

1. Introduction

Aerogels are materials with wide and varied applications given their unique properties as mesoporosity, low density, low thermal conductivity, and high surface area (Vareda et al., 2017; Smirnova & Gurikov, 2017). These characteristics make them highly useful in thermal insulation, packaging, and biomedicine (Venkataraman et al., 2016; Maleki et al., 2016). These materials are typically created from inorganic compounds such as silica; however, several organic compounds have been used in their formulation in recent decades, improving their biodegradability and biocompatibility (Zhu, 2019).

The production steps of the aerogels are widely known, and they are mostly formulated applying the sol-gel method in which a material that can create tridimensional networks is gellified to create a hydrogel. The hydrogel undergoes a drying process that substitutes the liquid within the material for a gas while keeping the porous structure intact (Dogenski et al., 2020; Kistler, 1931). Several drying techniques have been implemented in their formulation. Among them is supercritical drying (SCD) with CO₂, an inert and non-toxic gas with easily achievable supercritical properties, that allows the creation of aerogels with good porosity properties. This drying technique requires performing a solvent exchange, through which the water contained in the hydrogel is displaced by a solvent (usually ethanol) that is miscible with CO₂.

The supercritical conditions of CO₂ can be reached at 45 °C and 200 bar (De Marco et al., 2015); still, the costs of the equipment for supercritical drying are high. Additionally, adapting systems to maintain these conditions without the right equipment might lead to the release of CO₂ into the environment, contributing to environmental pollution. Among other drying techniques implemented, freeze drying produces hydrogels that undergo low temperatures, so the solvent can be evaporated in vacuum conditions. This results in porosities with a morphology characteristic of these materials and created by the water crystals in the tridimensional network (El-Naggar, 2019; Jiménez-Saelices et al., 2017). Vacuum drying (VD) has been used before due to its low energy consumption. It produces materials that commonly show pores of large size and a reduced surface area (El-Naggar, 2019).

Starch is an abundant biopolymer widely bioavailable that can be extracted from vegetable sources such as tubers, fruits, and cereals. Its characteristics and properties largely depend on the extraction source (Cornejo-Ramírez et al., 2018; Tester et al., 2004). Among the most relevant properties of rice starch (RS) are the small granule size and polyhedral morphology. Several rice varieties with designation of origin are found in Morelos, Mexico (Gallardo, 2018). To provide an added value to this specific rice variety, this work proposes to study the behavior of this starch in the creation of aerogels. In this work we seek to study the formation parameters of aerogels such as

concentration (8, 10, and 12% w/v) and retrogradation time (2, 4, and 6 days) implementing vacuum drying (Figure 1) and determine the most promising conditions. This technique is used to prove its feasibility, effectiveness, affordability, and versatility against supercritical drying to create starch aerogels. The aerogels obtained were partially characterized using Fourier transform infrared spectroscopy (FTIR), evaluating their morphology by scanning electron microscopy (SEM). Their thermal properties were assessed by differential scanning calorimetry (DSC), while the linear shrinkage (LS), moisture content (MC), swelling power (SP), water absorption capacity (WAC), and solubility (%S) were also identified.

2. Materials and methods

Rice from the “Soberano” brand was used for starch isolation. Acetone (99%) (CAS 67-64-1) was acquired from Karal. Sodium hydroxide (NaOH) (CAS 1310-73-2) and hydrochloric acid (HCl) (CAS 7647-01-0) were purchased from Supelco and Mayer brands respectively.

2.1. Rice starch isolation

Rice starch was isolated by alkaline hydrolysis using the method reported by Palma (2012) and Patindol et al. (2007), with modifications to fit our lab equipment. The rice was submerged in 1:4 NaOH (0.1 M) for 24 h. The mix was ground for 4 min in an Oster blender (Model 6844-000-N01) and sieved through 50 and 100 mesh. The yellow layer formed after each sieving was discarded. The pH was adjusted to 6.5 with HCl (0.2 M) and the mix was sieved through 200 mesh before washing several times with distilled water. The mixture was left standing for 24 h to eliminate the supernatant before centrifugation at 1000 rpm (112 relative centrifugal force) for 5 min in a centrifuge (model 800D, ZEIGEN). The precipitate was dried in a convection oven at 40 °C for 24 h.

2.2. Preparation of rice starch aerogels

The aerogels were prepared following the sol-gel technique described by several authors (Druel et al., 2017; Ubeyitogullari et al., 2018). Aqueous dispersions of rice starch were prepared at different concentrations (8, 10, and 12% w/v) and kept under mechanical agitation at 900 rpm and 90 °C for 50 min. The gelatinized dispersion was subjected to autoclave temperature and pressure (121 °C, 15 psi) for 20 min. The dispersion was stored in cylindrical containers kept under refrigeration (4 °C); starch was retrograded for 2, 4, and 6 days. A solvent exchange was carried out using acetone to facilitate its evaporation during drying. The hydrogel monoliths were cut to a 5 mL volume and submerged in a 50% acetone solution. The process was performed gradually to avoid contraction of the gel and the solvent was replaced every 24 h, increasing acetone concentration to 75% and 100%. The vacuum drying was carried out in a vacuum oven (model VA1, SHEL LAB) with a KNF

Lab pump. The samples in Petri dishes were placed inside the oven with excess acetone to prevent acetogel shrinkage when exposed to the environment. The samples were kept at a pressure of 20 inHg and a temperature of 40 °C until the solvent was completely removed from the vacuum chamber (4 h approximately).

The materials obtained are named according to their days of retrogradation, followed by the acronym for rice starch aerogels (RSA) and by the starch concentration used. Then the sample with 4 days of retrogradation and an 8% concentration is called 4D-RSA-8%, for the 10% sample it will be 4D-RSA-10%, and the 12% sample is then 4D-RSA-12%.

2.3. Linear shrinkage

The LS was calculated according to the report by Raman et al. (2015), monitoring changes in dimension of the materials after drying. The diameter of the cylindrical mold of the hydrogels was measured along with that of the dried aerogels. The calculation was done with the following equation:

$$LS = \frac{D_{Mold} - D_{Aerogel}}{D_{Mold}} \times 100\% \quad (1)$$

2.4. Functional characterization

The MC of the samples was calculated following the AOAC method 925.10. (Perez-Pacheco et al., 2014). The powdered aerogels (500 mg) were weighed in plates previously dried. They were then dried in a convection oven at 105 °C for 24 h to obtain a constant weight. The MC was obtained with the following calculation.

$$MC = \frac{(\text{Initial sample weight (g)} - \text{Dry sample weight (g)}) \times 100}{\text{Initial sample weight}} \quad (2)$$

The methodology by Ozturk et al. (2009) and Ubeyitogullari and Ciftci (2016) was implemented to evaluate SP, water solubility, and WAC. The dried aerogel and starch samples were submerged in distilled water and mixed in a vortex mixer for 30 s and heated in a water bath at 60 °C for 30 min with constant agitation in a magnetic stirrer. The tubes were then centrifuged at 4500 rpm (2268 RCF) for 15 min. The supernatant was decanted into Petri dishes (60 mm), and the weight of the precipitated gel was recorded. The supernatant and gel were dried in the oven at 105 °C for 24 h. Calculations were done using the following formulas.

$$SP = \frac{\text{Gel weight (g)}}{\text{Sample weight (g)} - \text{Soluble solid weight (g)}} \quad (3)$$

$$S\% = \frac{\text{Soluble solid weight (g)}}{\text{Sample weight (g)}} \times 100 \quad (4)$$

$$WAC = \frac{\text{Gel weight (g)} - \text{Dry gel weight (g)}}{\text{Sample weight (g)}} \times 100 \quad (5)$$

2.4. Physicochemical characterization

A FTIR analysis was carried out on Perkin Palmer equipment (Spectrum Two). The powdered aerogel samples were placed on the spectrophotometer lens, and the readings were done at the wavelength range 4000–600 cm⁻¹. The aerogel samples were coated with gold by turbomolecular-pumped sputtering in a thin film deposition unit (model Desk V, DENTON VACUUM). They were observed in a scanning electron microscope (model JSM-6010LA, JEOL). A DSC study was carried out in a TA Instruments equipment (model DSC Q2000) and a cooling module of the same brand. The sample (2 mg) was placed on hermetically sealed aluminum pans with 7 µL ultra-pure water. Samples were subjected to a nitrogen flow rate of 50 mL/min, and these were carried from 25 to 150 °C at a heating rate of 10 °C/min.

2.5. Statistical analysis

The statistical analysis of the data was carried out using Minitab 18 software with a 2-factor design (concentration and retrogradation). A one-way analysis of variance (ANOVA) was carried out with 0.05 significance, using a sample size n=3, and a general linear model to compare means.

3. Results and discussion

3.1. SEM

The comparison of the images obtained from the aerogels with different concentrations and retrogradation times and the aerogel morphology are shown in Figure 2. With 2 days of retrogradation, open areas with large spaces are observed. With the increase in days, it is possible to observe a greater amount of mass and the presence of some conglomerates. At 6 days of retrogradation, the gels show a larger pore size and some lump structures, while those that underwent 4 days of retrogradation showed homogeneous structures and more defined pore sizes. This behavior can be associated with the fact that during retrogradation, the starch molecules cross-link to return to their original structure, associating with each other and generating this morphology.

When the concentration in the aerogels is increased, the structures appear denser and can be observed an apparent increase in the thickness of the pore walls at all retrogradation days with a 12% starch concentration. De Marco et al. (2015) reported that the morphological change in aerogels depends on the starch source used, since potato and maize starches showed no changes in their morphology when increasing from 5 to 15% w/w, while 15% wheat starch produced xerogels with a lenticular structure. Besides, aerogels obtained using other biopolymers have shown the presence of interconnected structures through cell walls, such as those reported by Ozen et al. (2021) where they used medium molecular weight chitosan and microcrystalline cellulose in obtaining these materials.

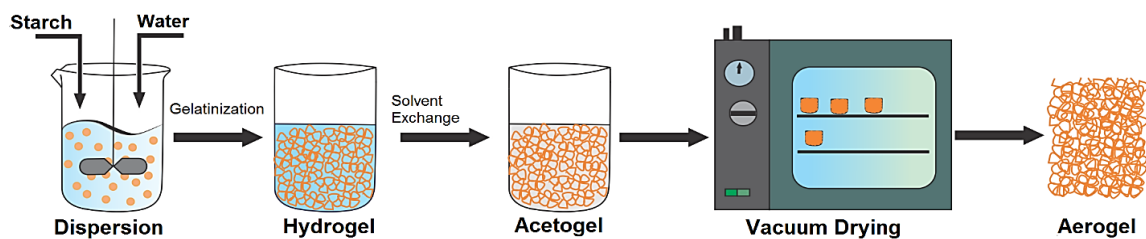


Figure 1. Diagram of the process for obtaining starch aerogels.

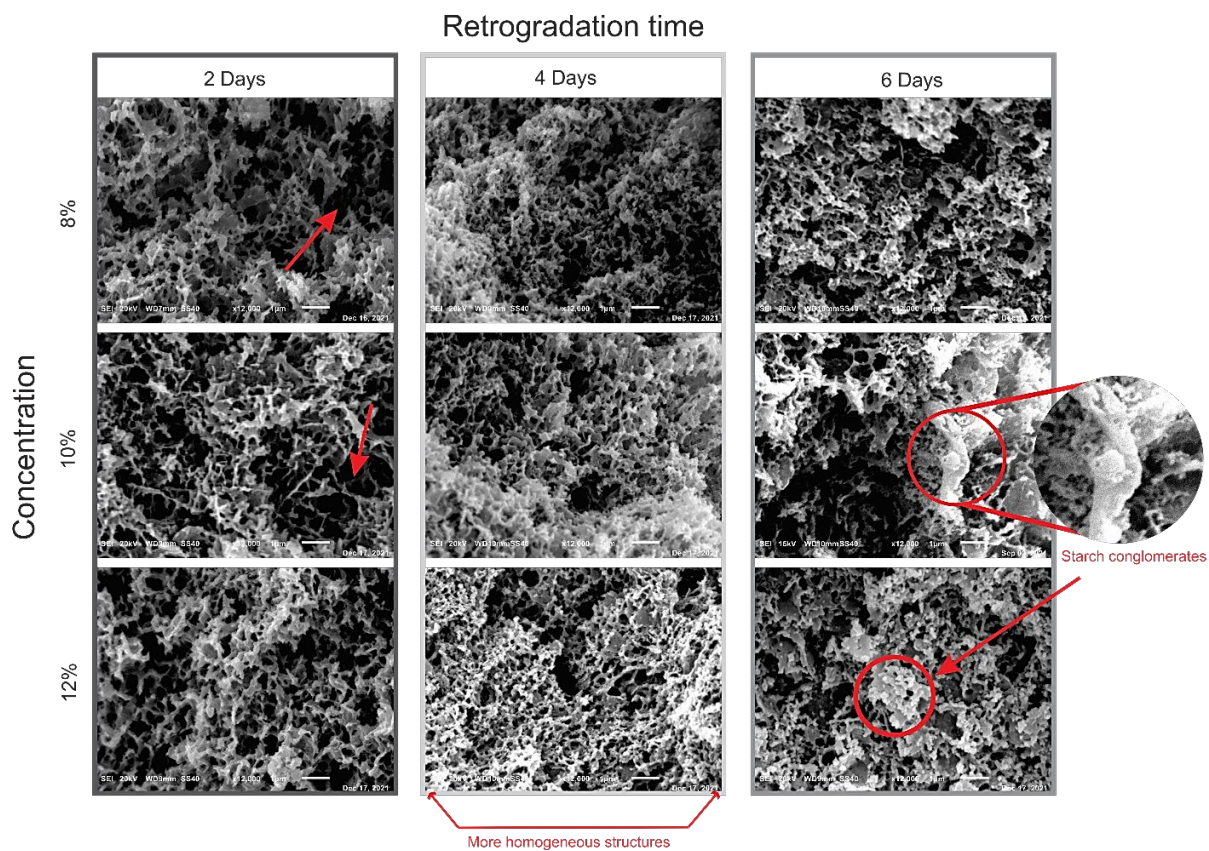


Figure 2. Micrographs of rice starch aerogels with different concentrations (8, 10, and 12%) at different retrogradation time (2, 4, and 6 days).

The pores were measured to obtain the means shown in Figure 3. The figure presents the tendency of these materials according to the starch concentration and retrogradation days as well as the minimum pore size measured at every concentration (%). The average pore size in aerogels at day 4 of retrogradation is smaller but it increases in aerogels at 6 days. A similar behavior is present when increasing the concentration (%) of rice starch. The samples with 4 days of retrogradation and a concentration of 10% (4D-RSA-10%) showed the smallest pore size (41 nm diameter) and an average of 77 nm. Ubeyitogullari and Ciftci (2016) obtain wheat

starch aerogels by supercritical drying with an average pore size of 20 nm. They observed this property is related to the surface area (53.5, 59.7, and 52.6 m²/g in samples prepared with 5, 10, and 15% wheat starch, respectively). They found no relationship between the concentration and the specific surface area of the aerogels. El-Naggar et al. (2020) describes that vacuum drying contributes to the collapse of the aerogel molecular structure, producing pores of large size. However, the use of vacuum drying in this work did not lead to the collapse of the structures, but instead generated materials with nanometer-sized pores. This demonstrates that it is possible to produce rice starch aerogels under this process.

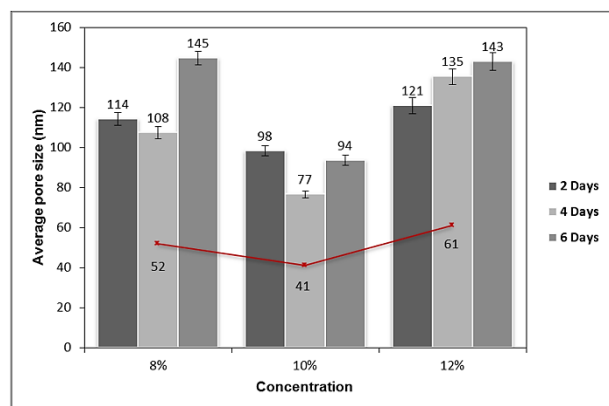


Figure 3. Histograms with pore size distribution in rice starch aerogels at different concentrations and retrogradation days (bars). The minimum pore size was measured by concentration percentage (line).

García et al. (2018) obtained an average pore size of 20–44 nm in materials produced from the carbonization of starch aerogels with graphite (20% w/w). Tran et al. (2020) obtained a rice straw – PVA aerogel sample by Freeze Drying with smaller pore sizes (10-20 μm). These authors use select binders to provide and enhance extensibility and strength of the 3D structure of the aerogels, but the results show no negligible difference. Even when the rice starch aerogels show a larger pore size and wide distribution that those dried by other more conventional methods such as the SCD with CO_2 , the vacuum drying process compensates for that disadvantage. In addition, the smallest pore size observed in the aerogels of this work is close to the reports by authors using supercritical drying.

3.2. FTIR

The spectra obtained from the FTIR analysis are shown in Figure 4. The comparison was made according to the percentage of concentration in the aerogels since the increase in the days of retrogradation shows a similar behavior and caused no significant changes in the FTIR spectra. Then, the characteristic peaks of starch are observed at 900–1200 cm^{-1} , attributed to the stretching of C-O and C-H bonds. The signals represent the presence of glucose (Mohammadi & Moghaddas, 2020), and the intensity of the peaks in the wavenumber range 1047–1022 cm^{-1} is related to the starch crystallinity (Smits et al., 1998; Salgado-Delgado et al., 2022). The peak located in the 1600 cm^{-1} region has been described in previous works as a result of the bending and stretching of the OH groups in the hydrogen bridges in water (Qin et al., 2016). Therefore, it has been linked to the moisture adsorbed in the materials and has been attributed to an increase in the specific surface area of nanomaterials (Maiti et al., 2013). Additionally, signals are in the wavelength 3300 cm^{-1} , indicating tension in the -OH groups, mostly associated to hydrogen bridges. Zhang et al. (2013)

stated that the bands at 1020 cm^{-1} are sensitive to changes in starch crystallinity, while the signal at 3400 cm^{-1} can show changes due to a reduction or increase in the amorphous region in the chain structure of this polysaccharide. Qin et al. (2016) obtained starch nanoparticles by thermal modification. They observed a loss of crystallinity as well as a decrease in intensity and a change in the wave number of the major signals in the infrared spectrum of the starch. These authors say that this change might suggest stronger bonds between the starch chains. The longer signals were obtained at a concentration of 10% starch, but they were reduced in the 8 and 12% samples. Although this behavior was not cited by the authors, it is suggested that aerogels with 10% starch tended to reorganize in a crystalline manner. Therefore, it can be said that, at this concentration, the parameters for the preparation of aerogels promote the reorganization of the starch chains during retrogradation. The 8% samples do not develop such reorganization since the amylose content in the aerogels is lower. Meanwhile, in the 12% samples there is a higher amount of starch, so factors as agitation or temperature are likely inadequate for promoting starch retrogradation.

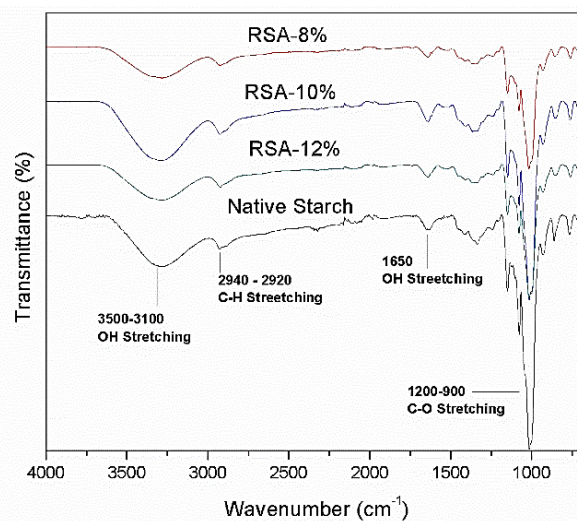


Figure 4. Infrared spectrum of native starch and rice starch aerogels (RSA) at different concentrations (8, 10 and 12%)

3.3. DSC

Figure 5 shows the comparison between gels with different starch concentrations and retrogradation days. After the thermal treatment, there was a loss of crystallinity in the starch responsible for creating a change in the latent crystallization energy (Figure 5A). It must also be noted that there is a displacement in the peak (shown in the diagram), indicating that the glass transition of the amorphous part of the starch as retrogradation days increase. This could be linked to the fact that longer times of refrigeration are related to an amorphous reorganization of the macromolecules forming the starch and

can be observed in 4 and 6 days of retrogradation samples (Figure 5B). Karlsson and Eliasson (2003) reported thermograms of potato starch from different tuber tissues subjected to gelatinization and refrigeration. They observed that, after 3 days of retrogradation, the starch tended to recover its crystallinity properties. However, in this work, the aerogels did not show such degree of reorganization.

On the other hand, there is a clear increase in enthalpy and the temperature required for T_g in 10% concentration samples (2D-RSA-10%) vs 12% samples (2D-RSA-12%). This means 10% aerogels tend to show better reorganization properties, both crystalline and amorphous).

Qin et al. (2016) suggest that the reduction in enthalpy required could be associated to the susceptibility of the structure to be destroyed after gelatinization. This could indicate that as the refrigeration days increase in obtaining aerogels, more stability is created in the amorphous region of the starch.

3.4. Linear shrinkage

The results of the calculation of LS in the aerogels are presented in Table 1. The vacuum-dried rice aerogels showed

caused by the change of solvent and drying applied showed a tendency to decrease as the starch concentration was higher along with the retrogradation days (Figure 6). However, no significant statistical difference was found between retrogradation days ($p > 0.05$) which could indicate that this factor does not have a direct effect on the degree of contraction of aerogels. Raman et al. (2015) produced hybrid aerogels from crosslinked alginate and different metallic carbonates, which presented a LS of 25–36%. This was attributed to the affinity of alginate to different cations. On the other hand, starch aerogels created by SCD have shown lower LS percentages, as observed in the work by Ubeyitogullari and Ciftci (2016). They found a volumetric shrinkage of 15.3% in aerogels with a starch concentration of 15%, then the contraction decreased as the concentration percentage increased. A similar behavior was observed in this work in terms of concentration. Dogenski et al. (2020) reported a volumetric shrinkage of 43–53% in hybrid starch-agar aerogels. They stated that this parameter can be used as a macroscopical indicator of the stability of the aerogel porous matrix during the production of the aerogels.

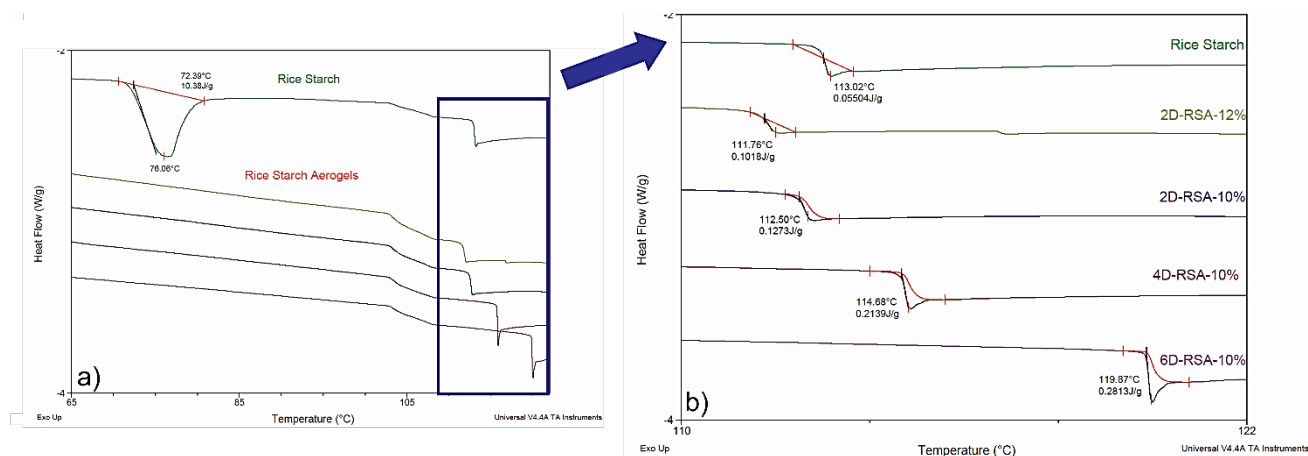


Figure 5. DSC diagram of native rice starch and rice starch aerogels at different concentrations (10% and 12%) and retrogradation times (2, 4 and 6 days) in a temperature range from a) 65 to 120 °C and b) 110 to 122 °C.

Table 1. Shrinkage percentage for rice starch aerogels.

Starch concentration	Linear shrinkage (%)		
	Retrogradation days		
	2D	4D	6D
8%	43±2 ^{ba}	36±1 ^{aA}	38±2 ^{ba}
10%	40±1 ^{abA}	37±2 ^{abA}	38±3 ^{abA}
12%	37±3 ^{aA}	37±2 ^{ba}	37±1 ^{aA}

Means ± SD.

Means that do not share a lower-case letter between lines are significantly different.

Means that do not share an upper-case letter between columns are significantly different.

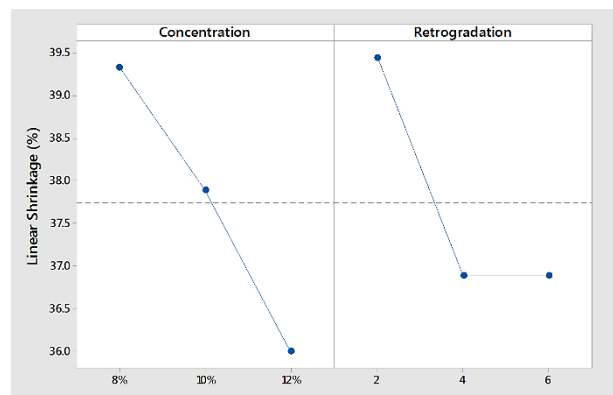


Figure 6. Main effects of the experimental design for the shrinking percentage of rice starch aerogels.

3.5. Moisture content

The data obtained for the MC in the aerogels are shown in Table 2. The amount of moisture in the aerogel samples increases along with the retrogradation days and starch concentration. The highest was 12% for the 6D-RSA-12% sample, while the lowest was 7% for 4D-RSA-8% and 6D-RSA-8%. The MC in the aerogels showed no significant statistical differences when increasing the retrogradation days, as we can see in Figure 7 this factor does not represent an interaction for this property and the starch concentration was the most influential. De Marco et al. (2015) obtained starch aerogels by SCD with 14% moisture. In contrast Mehling et al. (2009) detected 2.5% of residual moisture in potato starch aerogels and observed that the capacity of the aerogels to absorb moisture from the environment affects the measurement of certain parameters as surface area.

Table 2. Moisture percentages in rice starch aerogels.

Starch concentration	Moisture content (%)		
	Retrogradation days		
	2D	4D	6D
8%	8±0 ^{BA}	7±1 ^{BA}	7±1 ^{BA}
10%	8±1 ^{BA}	9±1 ^{BA}	12±1 ^{BA}
12%	10±1 ^{BA}	11±2 ^{BA}	12±2 ^{BA}

Means ± SD

Means that do not share a lower-case letter between lines are significantly different.

Means that do not share an upper-case letter between columns are significantly different.

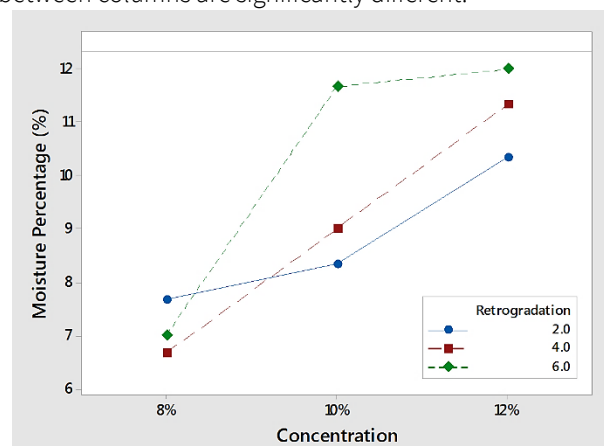


Figure 7. Interaction for moisture content in rice starch aerogels.

3.6. Interaction with water

The SP, WAC, and S% of the aerogels obtained can be seen in Figure 8. The highest swelling and absorption (17 and 14%, respectively) were observed under the conditions of 2 day and 8% concentration. The statistical analysis proved that retrogradation showed no significant statistical difference in WAC, while in SP the change is very small in 4 and 6 days of retrogradation (Figure 8b). Then, the absorption and swelling properties were mostly affected by concentration since when increasing this factor, a decrease of WAC and SP is observed (Figure 8a).

Dogenski et al. (2020) obtained a WAC of 200% hybrid agar-starch aerogels after 24 h at room temperature. They observed that the increase in OH groups promoted water interaction, while the dense microstructure could prevent water from entering the aerogel pores. da Silva et al. (2020) found that a higher tendency towards swelling, and water absorption promote the controlled release of active compounds and lead to the elimination of liquids accumulated inside food and drug containers. Additionally, they reported that polymer crystallinity affects these properties. Then, relating the structural change in the starch observed in the FTIR spectra (Figure 4), the samples with 8% w/v of starch seem to have the lowest crystallinity but the best water interaction properties. In contrast, the 10% samples showed the lowest swelling and water absorption values. A similar behavior was observed in the work by Camani et al. (2021) in crosslinked corn starch aerogels. They related the increase in the crosslinking agent to a reduction in WAC, stating that such changes were visible in the FTIR spectra of the aerogels.

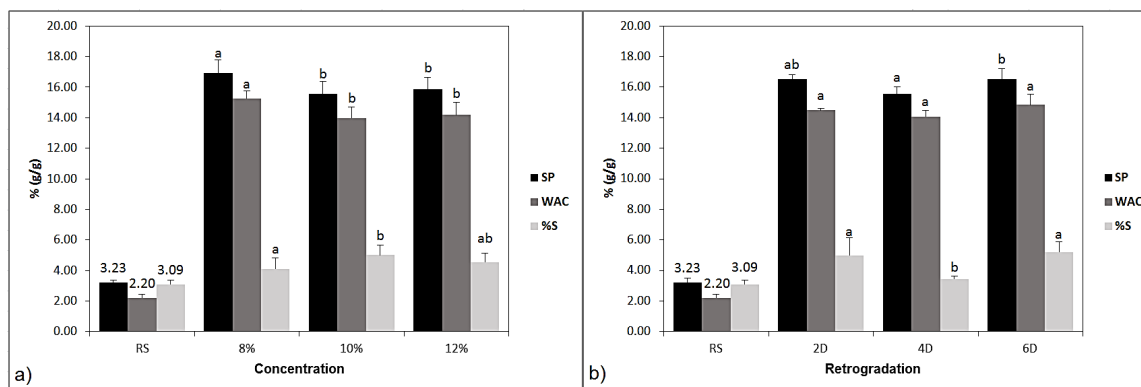


Figure 8. Swelling power (SP), water absorption capacity (WAC), and solubility (%S) of aerogels and native rice starch (RS) at different concentration percentages (a) and retrogradation time (b). Same color bars not sharing lower-case letters are statistically different.

The aerogel solubility, in Figure 8, allows to see that 10% w/v samples showed a better solubility vs 8% samples ($p < 0.05$); still, they did not present significant differences against 12% samples; then, the percentages were 5, 4.10, and 4.53, respectively. On the other hand, the aerogels reduced their %S to 3.44 at day 4 when compared against samples at 2 and 6 days (S% of 4.98 and 5.21, respectively) ($p > 0.05$).

Ubeyitogullari and Ciftci (2016) obtained lower S% values in wheat starch aerogels; the highest was 2.7% while S% increased along with the amorphous part of the sample.

4. Conclusions

The vacuum drying technique implemented in this work allows us to obtain affordable mesoporous aerogels in a practical and accessible way. The aerogels presented pores with diameters of up to 41 nm. It was determined that the increase in the days of retrogradation in the production of aerogels does not favor the formation of pores, in addition to not generating a significant decrease in linear contraction or improving the properties of interaction with water. Additionally, concentration is likely the major factor to study in future studies, evaluating several parameters during the process to obtain vacuum-dried aerogels. The samples with 10% starch presented the smallest pores and a better reorganization on all days of retrogradation. According to the FTIR spectra, there is evidence of a greater surface area at this concentration, in addition to the fact that it presents a greater solubility.

The aerogels produced from A98 rice starch in this work are biodegradable and biocompatible. In addition, their production does not involve the use of toxic reagents or pollutants; then, the technique is part of green chemistry. Among the potential uses of vacuum-dried aerogels, thanks to their increased water absorption and high porosity are applications in packaging, biomedicine, and the pharmaceutical sector.

Conflict of interest

The authors have no conflict of interest to declare.

Acknowledgements

A special recognition to the academic body of postgraduate studies and research of the INSTITUTO TECNOLÓGICO DE ZACATEPEC for the support granted in its facilities.

Funding

This work was supported by the “Consejo Nacional de Ciencia y Tecnología”.

References

- Camani, P. H., Gonçalo, M. G., Barbosa, R. F., & Rosa, D. S. (2021). Comprehensive insight of crosslinking agent concentration influence on starch-based aerogels porous structure. *Journal of Applied Polymer Science*, 138(34), 50863. <https://doi.org/10.1002/app.50863>
- Gallardo, R. A. C. (2019). *Propuesta de estrategias innovadoras para la comercialización de la denominación de origen del arroz del estado de morelos. caso: la perseverancia, Jojutla Morelos. [Tesis Maestría]. Instituto de investigación de Ciencias Básicas y Aplicadas, Centro de Investigación en Ingeniería y Ciencias Aplicadas UAEM, Cuernavaca, Morelos.*
- Cornejo-Ramírez, Y. I., Martínez-Cruz, O., Del Toro-Sánchez, C. L., Wong-Corral, F. J., Borboa-Flores, J., & Cinco-Moroyoqui, F. J. (2018). The structural characteristics of starches and their functional properties. *CyTA-Journal of Food*, 16(1), 1003-1017. <https://doi.org/10.1080/19476337.2018.1518343>

- da Silva, F. T., de Oliveira, J. P., Fonseca, L. M., Bruni, G. P., da Rosa Zavareze, E., & Dias, A. R. G. (2020). Physically cross-linked aerogels based on germinated and non-germinated wheat starch and PEO for application as water absorbers for food packaging. *International journal of biological macromolecules*, 155, 6-13.
<https://doi.org/10.1016/j.ijbiomac.2020.03.123>
- De Marco, I., Baldino, L., Cardea, S., & Reverchon, E. (2015). Supercritical gel drying for the production of starch aerogels for delivery systems. *Chemical Engineering Transactions*, 43, 307-312.
<https://doi.org/10.3303/CET1543052>
- Dogenski, M., Navarro-Díaz, H. J., de Oliveira, J. V., & Ferreira, S. R. S. (2020). Properties of starch-based aerogels incorporated with agar or microcrystalline cellulose. *Food Hydrocolloids*, 108, 106033.
<https://doi.org/10.1016/j.foodhyd.2020.106033>
- Druel, L., Bardl, R., Vorwerg, W., & Budtova, T. (2017). Starch aerogels: A member of the family of thermal superinsulating materials. *Biomacromolecules*, 18(12), 4232-4239.
<https://doi.org/10.1021/acs.biomac.7b01272>
- Tran, D., Nguyen, S., Do, N., Thai, N. N. T., Thai, Q., Huynh, H., ... & Phan, A. (2020). Green aerogels from rice straw for thermal, acoustic insulation and oil spill cleaning applications. *Materials Chemistry and Physics*, 123363.
<https://doi.org/10.1016/j.matchemphys.2020.123363>
- El-Naggar, M. E., Othman, S. I., Allam, A. A., & Morsy, O. M. (2019). Synthesis, drying process and medical application of polysaccharide-based aerogels. *International Journal of Biological Macromolecules*, 145, 1115-1128.
<https://doi.org/10.1016/j.ijbiomac.2019.10.037>
- García, A. M., Budarin, V. L., Zhou, Y., Hunt, A. J., Lari, L., Lazarov, V. K., ... & Shuttleworth, P. S. (2018). Monolithic mesoporous graphitic composites as super capacitors: From Starbons to Starenes®. *Journal of Materials Chemistry A*, 6(3), 1119-1127.
<https://doi.org/10.1039/C7TA09338A>
- Jiménez-Saelices, C., Seantier, B., Cathala, B., & Grohens, Y. (2017). Effect of freeze-drying parameters on the microstructure and thermal insulating properties of nanofibrillated cellulose aerogels. *Journal of Sol-Gel Science and Technology*, 84, 475-485.
<https://doi.org/10.1007/s10971-017-4451-7>
- Karlsson, M. E., & Eliasson, A. C. (2003). Gelatinization and retrogradation of potato (*Solanum tuberosum*) starch in situ as assessed by differential scanning calorimetry (DSC). *LWT-Food Science and Technology*, 36(8), 735-741.
[https://doi.org/10.1016/S0023-6438\(03\)00093-8](https://doi.org/10.1016/S0023-6438(03)00093-8)
- Kistler, S. S. (1931). Coherent expanded aerogels and jellies. *Nature*, 127(3211), 741-741.
<https://doi.org/10.1038/127741a0>
- Maiti, S., Jayaramudu, J., Das, K., Reddy, S. M., Sadiku, R., Ray, S. S., & Liu, D. (2013). Preparation and characterization of nano-cellulose with new shape from different precursor. *Carbohydrate polymers*, 98(1), 562-567.
<https://doi.org/10.1016/j.carbpol.2013.06.029>
- Maleki, H., Duřães, L., García-González, C. A., Del Gaudio, P., Portugal, A., & Mahmoudi, M. (2016). Synthesis and biomedical applications of aerogels: Possibilities and challenges. *Advances in colloid and interface science*, 236, 1-27.
<https://doi.org/10.1016/j.cis.2016.05.011>
- Mehling, T., Smirnova, I., Guenther, U., & Neubert, R. H. (2009). Polysaccharide-based aerogels as drug carriers. *Journal of Non-Crystalline Solids*, 355(50-51), 2472-2479.
<https://doi.org/10.1016/j.jnoncrysol.2009.08.038>
- Mohammadi, A., & Moghaddas, J. S. (2020). Mesoporous starch aerogels production as drug delivery matrices: synthesis optimization, ibuprofen loading, and release property. *Turkish Journal of Chemistry*, 44(3), 614-633.
- Ozen, E., Yildirim, N., Dalkilic, B., & Ergun, M. E. (2021). Effects of microcrystalline cellulose on some performance properties of chitosan aerogels. *Maderas. Ciencia y tecnología*, 23.
<http://dx.doi.org/10.4067/s0718-221x2021000100426>
- Ozturk, S., Koksel, H., Kahraman, K., & Ng, P. K. (2009). Effect of debranching and heat treatments on formation and functional properties of resistant starch from high-amylose corn starches. *European Food Research and Technology*, 229, 115-125.
<https://doi.org/10.1007/s00217-009-1032-1>
- Palma, H. (2012). *Caracterización de almidones de diferentes fuentes tratados con ácido para la encapsulación de vitamina C*. [Tesis Doctoral]. Instituto Politécnico Nacional, Centro de Desarrollo de Productos Bióticos, Doctorado en Ciencias en Desarrollo de Productos Bióticos. Yautepec, Morelos.

- Patindol, J. A., Gonzalez, B. C., Wang, Y. J., & McClung, A. M. (2007). Starch fine structure and physicochemical properties of specialty rice for canning. *Journal of cereal science*, 45(2), 209-218. <https://doi.org/10.1016/j.jcs.2006.08.004>
- Pérez-Pacheco, E., Moo-Huchin, V. M., Estrada-León, R. J., Ortiz-Fernández, A., May-Hernández, L. H., Ríos-Soberanis, C. R., & Betancur-Ancona, D. (2014). Isolation and characterization of starch obtained from *Brosimum alicastrum* Swartz Seeds. *Carbohydrate polymers*, 101, 920-927. <https://doi.org/10.1016/j.carbpol.2013.10.012>
- Qin, Y., Liu, C., Jiang, S., Xiong, L., & Sun, Q. (2016). Characterization of starch nanoparticles prepared by nanoprecipitation: Influence of amylose content and starch type. *Industrial Crops and Products*, 87, 182-190. <https://doi.org/10.1016/j.indcrop.2016.04.038>
- Raman, S. P., Gurikov, P., & Smirnova, I. (2015). Hybrid alginate based aerogels by carbon dioxide induced gelation: Novel technique for multiple applications. *The Journal of Supercritical Fluids*, 106, 23-33. <https://doi.org/10.1016/j.supflu.2015.05.003>
- Salgado-Delgado, A. M., Lozano-Pineda, E., Salgado-Delgado, R., Hernández-Uribe, J. P., Olarte-Paredes, A., & Granados-Baeza, M. J. (2022). Chemical modification of rice (*Oryza sativa*) and potato (*Solanum tuberosum*) starches by silanization with trimethoxy (methyl) silane. *Revista Mexicana de Ingeniería Química*, 21(3), Alim2802-Alim2802.
- Smirnova, I., & Gurikov, P. (2017). Aerogels in chemical engineering: Strategies toward tailor-made aerogels. *Annual review of chemical and biomolecular engineering*, 8, 307-334. <https://doi.org/10.1146/annurev-chembioeng-060816-101458>
- Smits, A. L., Ruhnau, F. C., Vliegthart, J. F., & van Soest, J. J. (1998). Ageing of starch based systems as observed with FT-IR and solid state NMR spectroscopy. *Starch-Stärke*, 50(11-12), 478-483. [https://doi.org/10.1002/\(SICI\)1521-379X\(199812\)50:11/12<478::AID-STAR478>3.0.CO;2-P](https://doi.org/10.1002/(SICI)1521-379X(199812)50:11/12<478::AID-STAR478>3.0.CO;2-P)
- Tester, R. F., Karkalas, J., & Qi, X. (2004). Starch—composition, fine structure and architecture. *Journal of cereal science*, 39(2), 151-165. <https://doi.org/10.1016/j.jcs.2003.12.001>
- Ubeyitogullari, A., Brahma, S., Rose, D. J., & Ciftci, O. N. (2018). In vitro digestibility of nanoporous wheat starch aerogels. *Journal of agricultural and food chemistry*, 66(36), 9490-9497. <https://doi.org/10.1021/acs.jafc.8b03231>
- Ubeyitogullari, A., & Ciftci, O. N. (2016). Formation of nanoporous aerogels from wheat starch. *Carbohydrate Polymers*, 147, 125-132. <https://doi.org/10.1016/j.carbpol.2016.03.086>
- Vareda, J. P., Lamy-Mendes, A., & Durães, L. (2017). A reconsideration on the definition of the term aerogel based on current drying trends. *Microporous and Mesoporous Materials*, 258, 211-216. <https://doi.org/10.1016/j.micromeso.2017.09.016>
- Venkataraman, M., Mishra, R., Kotresh, T. M., Militky, J., & Jamshaid, H. (2016). Aerogels for thermal insulation in high-performance textiles. *Textile Progress*, 48(2), 55-118. <https://doi.org/10.1080/00405167.2016.1179477>
- Zhang, H., Tian, Y., Bai, Y., Xu, X., & Jin, Z. (2013). Structure and properties of maize starch processed with a combination of α -amylase and pullulanase. *International Journal of Biological Macromolecules*, 52, 38-44. <https://doi.org/10.1016/j.ijbiomac.2012.09.030>
- Zhu, F. (2019). Starch based aerogels: Production, properties and applications. *Trends in Food Science & Technology*, 89, 1-10. <https://doi.org/10.1016/j.tifs.2019.05.001>